ARTICLE

A General Procedure to Functionalize Agglomerating Nanoparticles Demonstrated on Nanodiamond

Yuejiang Liang, Masaki Ozawa,* and Anke Krueger*

Institut für Organische Chemie der Julius-Maximilians-Universität Würzburg, Am Hubland, 97074 Würzburg, Germany

ABSTRACT Upon reduction of particle size to the nanometer range, one has to deal with the general issue of spontaneous agglomeration, which often obstructs postsynthesis modification of nanoparticle surfaces. A technique to cope with this phenomenon is required to realize a wide variety of applications using nanoparticles in solvents or as refined assemblies. In this article, we report on a new technique to facilitate surface chemistry of nanoparticles in a conventional glassware system. A beads-assisted sonication (BASD) process was examined to break up persistent agglomerates of nanodiamonds in two different reactions for simultaneous surface functionalization. The chosen reactions are the silanization with an acrylate-modified silane and the arylation using diazonium salts. The BASD process can be successfully applied even where the original material is not dispersible in the reaction solvent at all, as the formation of ever smaller, increasingly functionalized agglomerates is improving their solubility. We have confirmed that the presence of ceramic beads enables functionalization of each primary particle, while conventional magnetic stirring or beadless sonication can reach primary particles only when agglomeration is loose. Additionally, mechanical surface modification of nanodiamond was found to take place by BASD with high energy density, leading to sp^2-hybridized surface patches on nanodiamond. This allowed for the efficient grafting of aryl groups to the surface of primary diamond nanoparticles. Stable, homogeneously functionalized nanodiamond particles in colloidal solution can be obtained by this method.

KEYWORDS: nanodiamond · deagglomeration · surface chemistry · covalent · nanoparticles · attrition · colloids

The principal objective of nanotechnology is to build high-performance materials and devices having nanostructures. One of the major strategies is to use free-standing nanoparticles either dispersed in other media[1−3] or as building blocks of assemblies.[4,5] In both cases, tailoring of surface structures and properties is crucial in order to disperse these nanoobjects in solvents, to bind them to special functionalities, or to create chemical bonds to solid matrices. However, when particles become sufficiently small at the nanoscale, spontaneous agglomeration becomes more effective owing to the increasing influence of surface properties.[6,7] This makes surface chemistry crucial for nanoparticles. Contrary to soluble compounds, the aforementioned agglomeration hinders chemistry on them. Various attempts have been made so far to overcome this difficulty: covering with surfactants, polymers, *etc.*,[1,8−10] concurrent surface functionalization during particle growth,[11,12] and postsynthesis functionalization.[1,13−16] Most of them, especially those involving chemical reactions, can treat only dispersed particles throughout the entire process, leading to narrow potential ranges where electrostatic repulsive forces between charged particles counteract attractive forces.[17] In this context, conventional stirring methods do not produce sufficient energy density to break primary nanoparticles apart for surface functionalization. Therefore, new strategies to deagglomerate nanosubstances during chemical reactions are essential to perform a wide variety of reaction types.

There are several common deagglomeration techniques used for minute particles (mostly submicrometer particles) such as sonication,[18,19] high shear mixing,[20] mechanical milling,[21,22] and high-pressure processing.[23] Among them, owing to the easy handling, sonication is an energetic method suitable for chemical reactions especially of particles forming relatively weak agglomerates.[24] Higher energy density is required when attractive interparticle forces become more pronounced due to extremely small particle size, strong electrostatic forces, and/or covalent bonds. Stirred media milling is a burgeoning technique, which agitates micrometer-sized beads to induce high-energy impact and shear forces.[25−27] Functionalization in a mill has also been reported for specific cases.[28,29] However, integration of such a mill into the standard setups of chemistry with atmospheric and temperature control, use of toxic chemicals, irradiation, electrochemical treatments, *etc.*, remains technically demanding.

Recently, we disclosed a beads-assisted sonic disintegration process (BASD). This

*Address correspondence to krueger@chemie.uni-wuerzburg.de, masaki.ozawa@uni-wuerzburg.de.

Received for review April 3, 2009 and accepted May 27, 2009.

Published online July 14, 2009. 10.1021/nn900339s CCC: $40.75

method shows similar deagglomeration performance compared to stirred media milling, just by additionally charging ceramic beads to a sonicated suspension.[30] As the technique is facile and adaptable, the BASD setup can be easily integrated in the conventional glassware systems to enable functionalization of primary nanoparticles even under conditions where particles are actually (re-)flocculating. Here, detonation nanodiamond (D-ND) sizing at around 4−5 nm[31,32] was employed as model nanoparticles. They feature typical properties, such as a surface suitable for chemistry, and notoriously persistent agglomerates (100−200 nm in size) unbreakable by intensive sonication.[30] The latter feature is considered to arise from covalent bondings[25,33] and/or extremely strong electrostatic attractive forces[34] on top of van der Waals forces. Here we demonstrate BASD as a key method pushing nanotechnology from the chemistry side by enabling surface functionalization of primary nanoparticles accompanied by deagglomeration, which is applicable not only to nanoparticles forming rather weak agglomerates such as synthetic monocrystalline nanodiamonds (SYP-ND) but also to agglomerated detonation nanodiamonds (D-ND), the extreme end of tight agglomeration.[25,31−33]

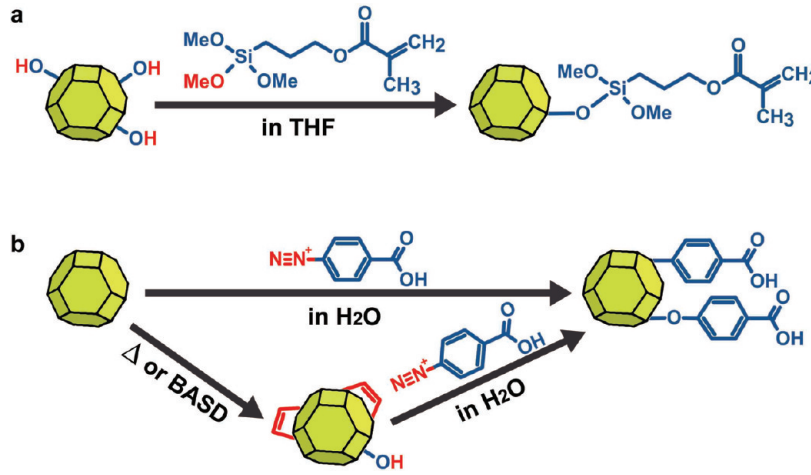

Scheme 1. Surface functionalization of nanodiamond. (a) Silanization of nanodiamond surfaces. A simple condensation reaction between hydroxyl groups and (3-acryloxypropyl)trimethoxysilane yields silanized nanodiamonds in dry THF. Hydroxylation was carried out on D-NDs by borane reduction prior to silanization.[35] On the other hand, SYP-NDs were found to carry enough hydroxyl groups without hydroxylation. The reaction requires inert atmosphere to avoid condensation with moisture. (b) Arylation of nanodiamonds by applying aromatic diazonium salts. They react with C═C or −OH groups after surface modification at high temperature or a BASD pretreatment. Note: The nanodiamond particles are depicted as truncated octahedrons here, as it is one of the suggested model structures for this material.[34,36] However, this is an idealized shape, and TEM images show rather roundish diamond particles and few pronounced facets in the case of D-ND.

RESULTS AND DISCUSSION

Two different reactions, that is, a simple condensation reaction leading to silanization and an arylation with diazonium salts, were performed on D-ND agglomerates to achieve surface functionalization on primary nanoparticles. The first takes place on OH groups,[35] while diazonium salts carrying aryl groups can additionally attack C═C bonds as portrayed in Scheme 1. Recently, a detailed discussion of the structure of nanoscale diamond has been published.[37] The authors used solid-state ^{13}C NMR and $^{1}H-^{13}C$ dipolar coupling to investigate the surface structure. They found a considerable amount of OH groups and only little amounts of sp^2 carbon at the nanodiamond surface.

The setup illustrated on the left side of Figure 1 was employed for reactions with BASD. In order to verify the effect of BASD, beadless sonication (BLS) and magnetic stirring (MS) were also examined for comparison. Since the sonication effect is subject to parameters such as kind and amount of solvent, shape of container, position of sonotrode, *etc.*, exactly the same configuration as for BASD was used for the BLS reactions. A round-bottom flask was used for MS.

Although D-NDs form relatively stable slurries in water, they flocculate and precipitate in most organic solvents (even when dispersed by powerful sonication) due to their hydrophilic character.[30] Borane reduction little affects this property.[35] Hence, silanization of borane-reduced D-NDs in tetrahydrofuran (THF) starts under flocculating conditions. Inert atmosphere was maintained during the entire process for all techniques

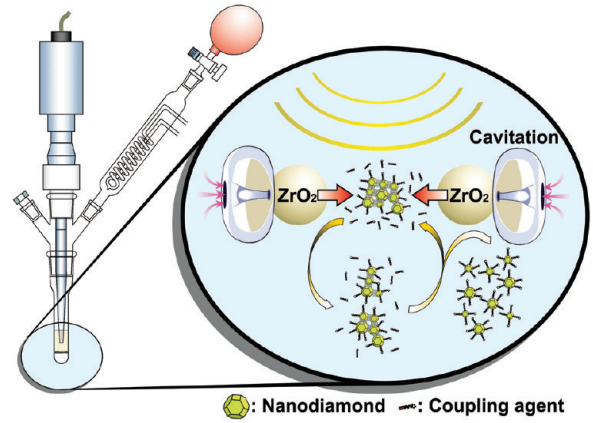

Figure 1. BASD setup for simultaneous surface functionalization and deagglomeration of nanoparticles. The setup was designed for chemical reactions using a powerful sonicator equipped with a horn-type sonotrode. An airtight environment is maintained by a commercial Teflon joint between the sonicator and a universal glass joint. The glass parts are composed of a lower tube reactor and an upper three-neck branch adapter, allowing for various chemical procedures. In the reactor, microjets and shock waves generated by implosion of ultrasonic microbubbles accelerate the ceramic beads. Breaking up of agglomerates is thought to take place owing to the impact and shear forces of the collisions between the sonically propelled beads. When the agglomerates are treated with coupling agents, freshly exposed surfaces react with the agents until all primary particles are deagglomerated and functionalized.

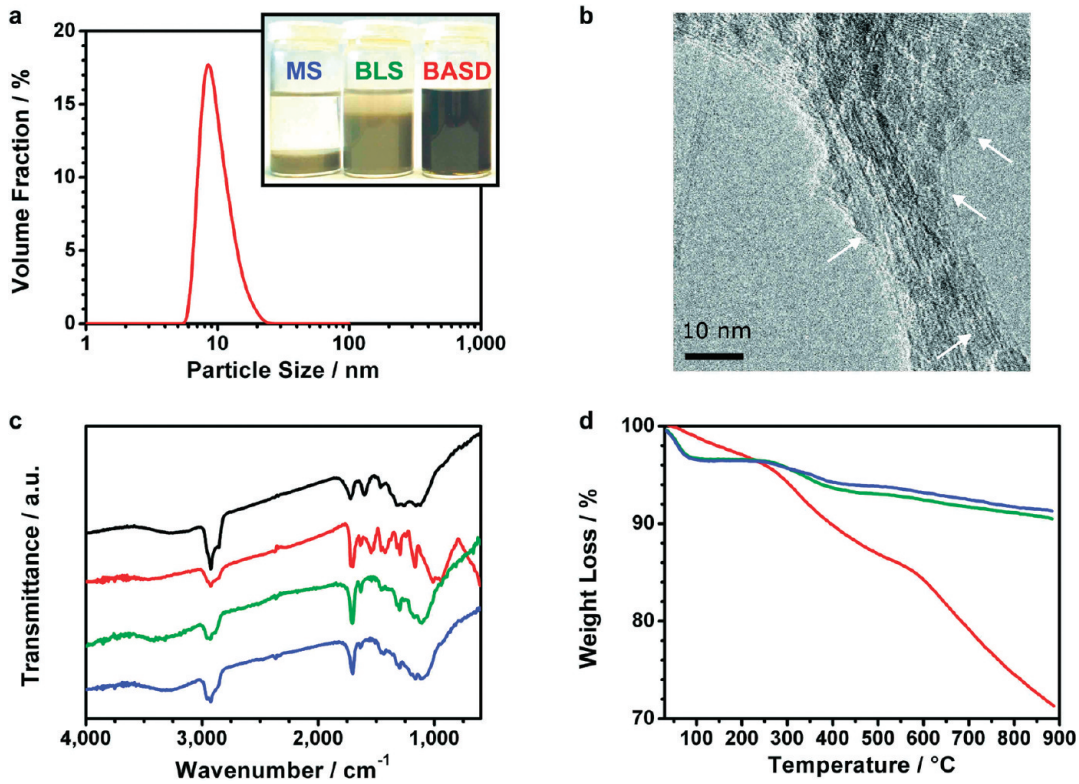

Figure 2. Characterization of D-NDs silanized using BASD (red), BLS (green), and MS (blue). (a) Dispersion behavior of the silanized samples in THF; pictures taken 150 min after shaking. While gray slurries obtained with BLS and MS settled down within an hour (hence no DLS measurement possible), the clear colloid resulting from BASD silanization showed no significant change over 5 months. Particle volume distribution of the colloid measured in THF by DLS presents the main peak at ~8 nm close to the size of the primary particles. Despite the similarity between BLS and MS samples, the former flocculated in a muddy way, and the latter formed granular agglomerates. (b) Typical HRTEM micrograph of the BASD-silanized D-NDs (see arrows for exemplary particles) deposited on SWCNTs in THF. The particles are quite homogeneously scattered with no pronounced agglomeration. The lattice fringes of the particles have ~0.2 nm interplanar spacings corresponding to diamond (111) planes. (c) FT-IR spectra of the pristine D-NDs (black) and silanized samples (red, green, blue corresponding to BASD, BLS, and MS, respectively). The features of the functional groups are observed most clearly in the BASD sample (red). (d) Thermograms of the silanized samples. The large weight loss of the BASD sample (red) corresponds to a surface loading much higher than for the other samples. The absence of water desorption at ~100 °C in the red trace is consistent with the resulting hydrophobic surfaces.

(MS, BLS, BASD) in order to avoid moisture-derived condensation. The particles stayed indispersive throughout the reactions except in the case of BASD, where nanodiamonds were gradually stabilized to give a deep brownish clear colloid (Figure 2a). The particle size of the BASD product determined in THF (a solvent where the starting material immediately precipitated) by means of dynamic light scattering (DLS) method was close to the size of the primary particles with functional groups (Figure 2a). HRTEM observations also verified deagglomeration of the diamond particles (Figure 2b). The isolated colloidal particles were too small for direct observation on a conventional copper grid coated with lacey carbon film, though, and reagglomeration occurred upon drying a drop of colloidal solution on the grid. Hence, the nanodiamond particles were preadsorbed onto bundles of single-wall carbon nanotubes (SWCNTs) in THF. Isolated nanoparticles settled on the SWCNTs, thus showing the newly acquired dispersibility in this rather nonpolar solvent. This also indicates functionalization of the primary D-ND particles.

The distinct effect of BASD was observed in the Fourier transform infrared (FT-IR) spectra as presented in Figure 2c. All silanized samples exhibit absorption bands corresponding to acrylate groups at 1700, 1635, 1300, and 1110 cm^{-1}, on top of the broad bands stretching around 3300 and 2950−2850 cm^{-1}, attributable to −OH groups and the C−H stretching vibration, respectively. The most notable difference between the methods was the remarkable downshift of those bands that represent the C−O−Si asymmetric stretching modes. These are observed at around 1110 cm^{-1} in the BLS and MS samples, while they are shifted to 1010−940 cm^{-1} with BASD. This is due to the mass effect: The free vibration of C−O−Si groups is influenced by the mass of the attached nanoparticle/agglomerate. The huge agglomerates in BLS- and MS-functionalized samples can be considered a static body, whereas the functionalized primary nanoparticles in the BASD sample with their much lower mass interfere with the functional group vibrations. A thermogravimetric analysis (TGA) revealed no adsorbed water in the

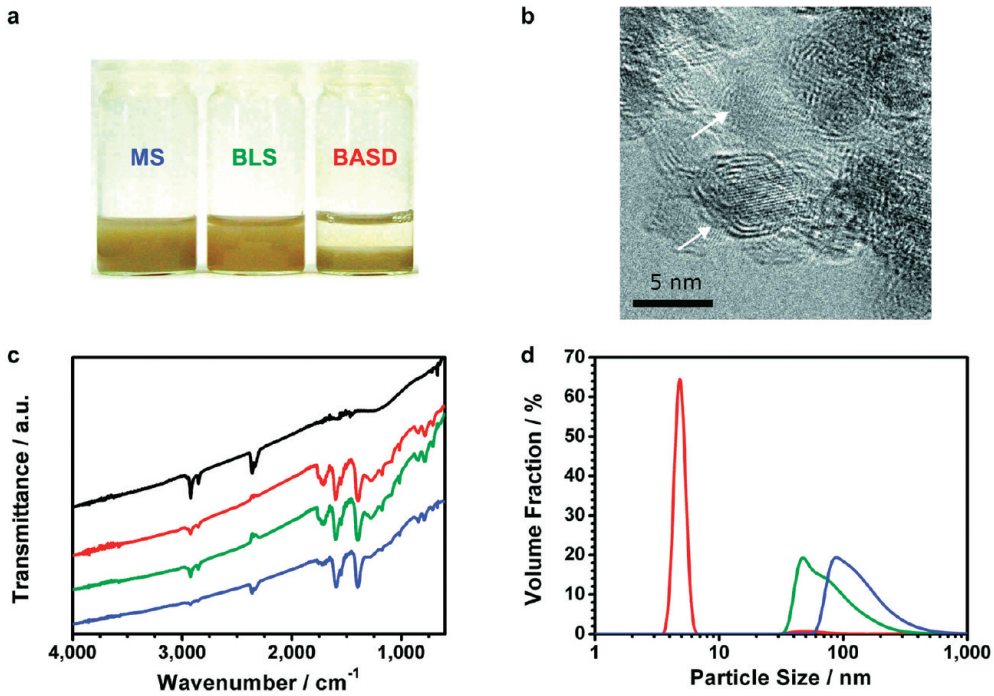

Figure 3. Characterization of D-NDs arylated using BASD (red), BLS (green), and MS (blue). (a) Dispersion behavior of the arylated samples in basic solutions (pH ~ 11, D-ND not pretreated, see below); pictures taken 1 h after shaking. The BLS and MS samples formed turbid brownish suspensions stable for a few hours, while the BASD-arylated sample precipitated within a few minutes. (b) HRTEM image of D-NDs annealed at 1100 °C *in vacuo* for 1 h, showing bucky nanodiamonds (see arrows). Completely transformed onions were also observed. (c) FT-IR spectra of the pristine D-NDs (black) and arylated samples after annealing at high temperature. (d) Particle volume distributions of the arylated samples after annealing measured in basic solutions by DLS at pH 10−11.

BASD sample, indicating a hydrophobic character of the surface (Figure 2d). Moreover, compared to the non-BASD samples, a remarkably increased weight loss was observed with a step between ~300 and 500 °C. Since the boiling point of (3-acryloxypropyl)-trimethoxysilane is 253 °C, it also supports the covalent bonding of 3-acryloxypropylsilyl groups to the nanodiamonds.

In contrast to silanization, arylation started with aqueous slurries of D-ND. However, addition of diazonium salts at 80 °C gave rise to immediate sedimentation accompanied by generation of gas and a color change from gray to red-brown within several minutes. The flocculation persisted throughout the reactions, showing no noticeable dependence on the methods. Dispersibility of the resulting products assumedly functionalized with benzoic acid groups (or −Ph−COO^- at higher pH) was similar to that of the pristine D-NDs. In most solvents, dispersibility was slightly weaker, as expected from the behavior of those samples functionalized oxidatively with carboxyl groups alone.[30] DLS measurements performed in dimethyl sulfoxide, which, to our knowledge, is the best solvent for D-NDs, revealed particle sizes of less than 10 nm for the BASD-arylated sample, while the other methods led to peaks at around 100 nm or more. Thus deagglomeration by BASD was demonstrated in DMSO. Still another solvent in which D-NDs disperse only *after* arylation should be employed to verify the successful functionalization. For instance, the arylated material should form stable solutions under basic conditions as the organic moieties are carrying COOH groups. In comparison, acid or air oxidation of D-NDs (to introduce carboxyl groups directly on the ND surface) induces a shift of the colloidal pH window from pH 3 to 6 toward basic conditions accompanied with a change of ζ potential from positive to negative. Similarly, the BLS and MS samples were found to be rather stable in basic aqueous solutions (Figure 3a). However, the BASD sample unexpectedly showed immediate sedimentation. In addition, it turned to a clear colloid under slightly acidic conditions, thus resembling the pristine D-NDs. All samples precipitated in water under neutral conditions.

The unexpected behavior of the arylated D-NDs in basic solutions might be due to the sparse −OH and C═C groups on the pristine surfaces of the true primary particles in the inner part of agglomerates, allowing only for sparse grafting of aryl groups. Therefore, a surface modification of those particles is required. Schmidt-Rohr and co-workers have recently discussed the structure modification induced by thermal annealing of ND.[37] By measuring solid-state ^{13}C NMR spectra, they proved the removal of OH groups and the appearance of sp^2 carbon at the diamond surface. In our work, D-ND was pregraphitized at 1100 °C for 1 h *in vacuo*, resulting in a mixture of bucky diamonds and some nano-onions (Figure 3b) as previously reported by Kuznetsov

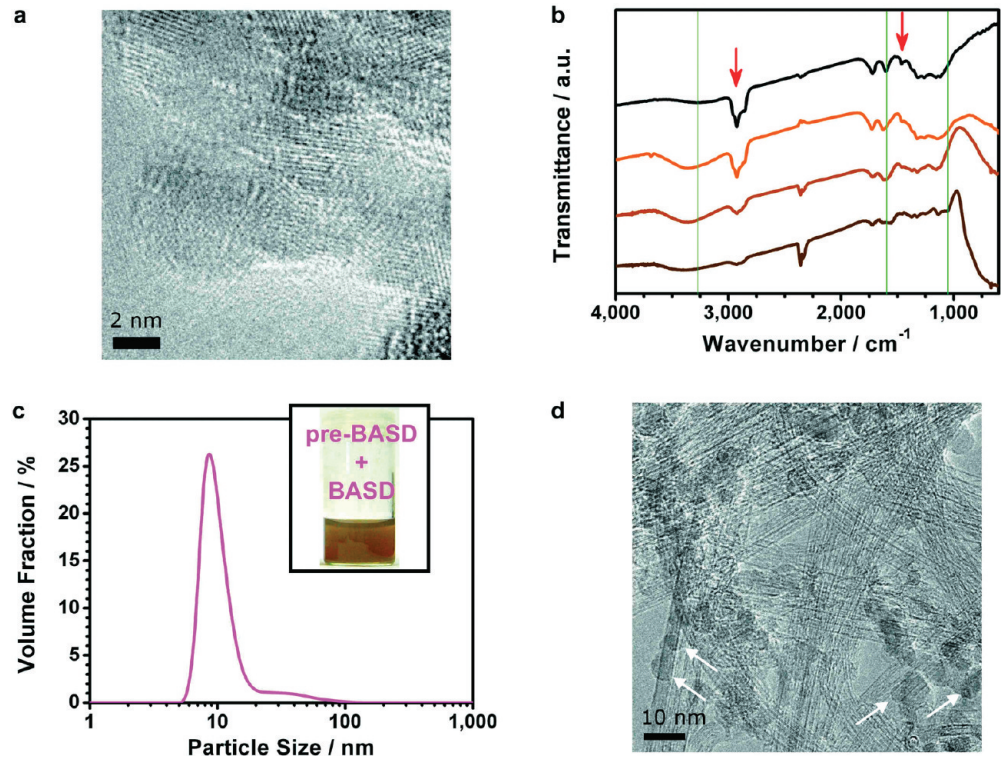

Figure 4. Arylation of D-NDs involving BASD pretreatment. (a) HRTEM image of D-NDs treated by BASD for 12 h at the maximum amplitude in water. No significantly graphitized surfaces were observed (while the diamond lattice is clearly visible). (b) FT-IR spectra of the pristine D-NDs (black) and the BASD samples treated for 3 h (pale brown), 6 h (brown), and 12 h (dark brown). Three green auxiliary lines as well as the red arrows emphasize the variation with time. (c) Aqueous colloid of the BASD-arylated D-NDs with the BASD pretreatment. Particle volume distribution was measured by DLS on the clear brownish colloid under slightly basic conditions at pH 8.5. The main peak at ~8 nm corresponds to the hydrodynamic diameter of the primary particles. (d) HRTEM micrograph of the BASD-arylated D-NDs with the BASD pretreatment deposited on SWCNTs in a basic aqueous solution. The particles having diamond (111) lattice fringes are homogeneously scattered with no pronounced agglomeration (arrows).

et al.[38] The powder was then allowed to react with the diazonium salts using all three methods. All reactions proceeded under flocculating conditions similar to those without pregraphitization. In all cases, the completely black products were considerably stable under basic conditions from pH 6 to 13 showing negative ζ potentials, with no significant variation depending on the method. At around pH 10, for example, BASD, BLS, and MS gave ζ potentials of −39, −45, and −43 mV, respectively. FT-IR spectra of them presented the features of the functional groups with insignificant differences depending of the methods (Figure 3c). In addition to the bands around 2900 cm^{-1} corresponding to saturated C−H bonds, strong absorption bands attributable to antisymmetrical and symmetrical stretching modes of carboxylates, respectively, were observed around 1595 and 1395 cm^{-1} together with the band at 1710 cm^{-1} corresponding to carboxyl groups. The weak peaks at around 790 cm^{-1} are attributable to aromatic rings. However, unlike the similar features seen in the spectra, DLS revealed 4.8 nm for the particle size of BASD-arylated D-NDs at the main peak of the narrow particle volume distribution—in sharp contrast to those at ~45 nm for BLS and ~80 nm for MS (Figure 3d). Thus, arylation of graphitized primary particles was achieved only with BASD.

Despite the success in arylating thermally annealed D-NDs, metamorphoses of the particle cores are nearly inevitable at high temperature. The stability of diamond surfaces depends on the crystallographic conditions of individual surfaces.[39] Therefore, yet another approach using BASD was examined: It makes use of the surface graphitization of nanodiamond likely induced by stirred media milling.[32,40,41] A prolonged BASD mechanical processing for 12 h did not give rise to microscopically detectable graphitic domains on nanodiamond surfaces (Figure 4a). However, FT-IR spectra presented some changes (Figure 4b). The strong absorption bands around 2900 cm^{-1} and the small band at 1465 cm^{-1} corresponding to saturated C−H bonds decreased or vanished with time. Growth of the broad band around 3360 cm^{-1} corresponding to −OH groups in hydrogen bonds occurred with a new band arising at around 1060 cm^{-1}, which is also attributable to these groups. Broadening of the band at 1600 cm^{-1} with additional peak at around 1560 cm^{-1} likely reflects formation of conjugated C═C

bonds and aromatic rings. The prominent drop of the transmittance below 970 cm^{-1}, which grows with processing time, seems to be mainly due to fragmented zirconia beads (see Supporting Information, Figure S5). Furthermore, a weakening of the broad bands around 1300 cm^{-1} was observed.

For the reaction, D-ND powder suspension was treated by BASD for 6 h prior to the addition of the diazonium salt. This pretreatment was found to improve colloidal stability of the BASD-arylated D-NDs considerably to give a clear colloid (Figure 4c). Particle sizes of less than 10 nm were observed at pH 8.5 with a negative ζ potential of -36 mV. This indicates the facilitated arylation due to the formation of the target moieties (here C═C and OH) during the pretreatment. HRTEM observations demonstrated homogeneous deposition of the particles on SWCNTs in a basic aqueous solution (Figure 4d), supporting both deagglomeration and functionalization (see Supporting Information, Figure S1, for more details).

We also examined the two model reactions on another type of nanoscale diamond (*i.e.*, SYP-NDs). They were commercially jet-milled after high-temperature high-pressure synthesis, oxidized to make the surfaces hydrophilic, and then graded (<50 nm, main peak at 35 nm, Van Moppes Corp.). Its most distinct feature from detonation nanodiamond is the considerably weaker agglomeration owing to the absence of interparticle covalent bonds, the larger size, and the random shapes. Despite the weak agglomeration in the starting material, after the silanization, only the BASD sample consisted of functionalized particles of ~35 nm that were dispersible in THF (see Supporting Information, Figure S2). In contrast, all of the arylated samples dispersed well in basic solutions (pH ~11) with particle sizes around 30 nm regardless of the stirring/deagglomerating methods (see Supporting Information, Figure S3). This difference between silanization and arylation might be attributed to strong influence of solvents on the interparticle forces.

Not only the analytical data but also the evident change in dispersing behavior of D-ND and SYP-ND after the reactions proves the functionalization. Grafting silanes or aryl groups on the true *primary* nanoparticles of D-ND or SYP-ND, however, was only obtained when BASD was employed (except for arylation of SYP-ND, where dispersibility was high even with conventional treatment). Thus, integration of this high-energy deagglomeration process in the conventional setups for wet chemistry can open the door to surface functionalization of primary nanoparticles of all kinds. Here we have chosen nanodiamond as an exemplary material as it combines a strong agglomeration and interesting surface chemistry. However, the technique is not limited to this material. Also, other agglomerating nanoparticles can be simultaneously deagglomerated and surface-modified.

The unexpected dispersing trend of the arylated D-ND samples without the pretreatment seemingly contradicts surface functionalization of primary particles with BASD. However, this finding can be interpreted as follows: The detonation process for D-ND production also generates graphitic byproduct during the cooling stage, which is usually removed oxidatively before further use. Nevertheless, the agglomerated structures are retained throughout the entire purification process. This gives rise to agglomerates carrying functional groups and regraphitized areas[39,42] only on their outer surfaces. The internal particle's surfaces are not affected by this treatment and thus carry much less functionality. When broken free from the agglomerates, those fresh surfaces are then much less reactive than the outer, oxidized surfaces of the original agglomerates. Hence, the particles originating from the cores of the agglomerates behave like pristine D-NDs. On the other hand, BLS and MS do not liberate the internal particles but yield somewhat functionalized agglomerates showing modified properties. This hypothesis is strongly supported by the functionalized primary nanodiamonds obtained from the pretreated D-NDs, which acquired strongly enhanced dispersibility.

It is still hard to envisage how exactly deagglomeration proceeds with BASD. However, it might be considered as illustrated in Figure 1. Although ultrasonic processors are powerful synthetic tools in liquid−solid chemical reactions involving deagglomeration or fragmentation, sonication alone may be insufficient in cases when interparticle bondings are too strong. However, microjets or shock waves induced by ultrasonic cavitations[43] can act as propelling vehicles of neighboring tiny objects. For instance, impact velocities between sonically accelerated metal particles of about 10 μm in diameter reach 500 m/s,[44] which is far beyond the peripheral speed of stirred media milling usually operated at around 10 m/s or less. Therefore, the presence of ceramic beads probably causes a high number of collision events, giving rise to milling effects. Considered this way, BASD is the first bladeless derivative of stirred media milling. Actually, the deagglomeration characteristics in BASD resemble stirred media milling rather than beadless sonication.[30] The mechanical stress, however, can be much greater, and the compatibility with wet chemistry processes is by far better.

In addition to the deagglomeration effect, prolonged BASD was found to induce a modification of nanodiamond surfaces. In the FT-IR spectra of the BASD-treated D-NDs, formation or reconstruction of C═C bonds was indicated as well as the formation of OH groups. This explains why D-NDs acquired high dispersibility in basic solutions when the BASD-pretreated D-NDs were arylated. As reported for stirred media milling,[32,40,41] impact and shearing forces of beads elevate local temperatures sufficiently to attain stable surface structures.[39,42] Hydroxylation took place presum-

ably owing to radical reactions with water.[28] In contrast to high-temperature treatment in a furnace, transformation induced by mechanical treatment is limited to the uppermost layers of the particles. Thus, pre-BASD is expected to render diamond surfaces suitable for further functionalization while retaining the core structures of the nanodiamonds.

BASD is presumably based on collisions of beads induced by cavitations. This sets guidelines for use: In order to achieve high efficiency, a solvent with high boiling point and low viscosity has to be chosen to prevent bubble generation and to allow high-speed movement of the beads, respectively. Dispersibility of nanoparticles in a solvent is an issue of interest in handling BASD. A reaction under flocculating conditions gives rise to an endless cycle of deagglomeration and reagglomeration. In this case, the chosen coupling agent must reach the target moieties on the freshly exposed surface and complete the reaction before reagglomeration. If this reaction stabilizes the particles in the respective solvent, agglomerates will become gradually smaller. Due to the surface stabilization by the functional groups, no (or almost no) reagglomeration occurs and the primary particles are eventually liberated. This is the case for silanization, where functionalized nanodiamonds were dispersed in THF. Arylation, on the contrary, causes no gain in dispersibility as the resulting surface groups do not alter the dispersion behavior. Still the present study proved surface functionalization of primary particles being achievable even under such unfavorable conditions.

Certain drawbacks of BASD should also be considered, such as contamination with bead and sonotrode fragments and damage on nanoparticles. The first is sometimes hard to remove by centrifugation because of nanoimpurities resulting from bead abrasion[30] (see Supporting Information, Figure S4). Such nanozirconia fragments can be removed using phosphoric acid at elevated temperature or concentrated NaOH solution.[32] Another possible solution is to employ other materials for the beads. Replacement of zirconia by silica beads, for example, gave similar milling results.[25] However, there are no equivalent substitutes for Ti alloy sonotrodes so far. Ti-derived impurities, although usually much less important than those from beads, must be removed using corrosive reagents. The damaging issue is more critical when brittle materials are processed. However, functionalization with BASD is achievable by adjusting the energy input, provided the interparticle bonds are weaker than the particles themselves. Therefore, parameters such as the amplitude of sonication and kind of beads should be optimized for each case, as reported for stirred media milling.[26] Furthermore, it should be noted that BASD might induce additional radical reactions as pointed out both for stirred media milling[28] and sonication,[45] which might result in unexpected products (*e.g.*, reactions with the solvent). Nevertheless, the simultaneous functionalization with BASD enables a wide variety of possible reactions on nanoparticle surfaces, including photochemistry and electrochemistry under inert conditions, due to the simple setup and procedures as demonstrated in this study.

CONCLUSION

In summary, we have developed a versatile and efficient method for the simultaneous deagglomeration and surface functionalization of strongly agglomerated nanoparticles applying a beads-assisted sonication technique. Here we have chosen nanodiamond due to its notoriously strong agglomeration resulting from several modes of interaction (electrostatic, covalent, hydrogen bonding, *etc.*). The method enables the production of functionalized nanoparticles consisting of the primary particles of the material. Even in media where the original particles are flocculating, an efficient functionalization takes place. The latter is leading to truly dispersed primary nanoparticles with a homogeneous surface termination. The method is applicable to all kinds of other agglomerating particles, provided the solvent and beads have been chosen appropriately. Test runs with metals, oxides, and carbon nanotubes have yielded promising results. More detailed investigations on the application to nondiamond materials showing strong agglomeration and to new surface modifications are underway and will be reported in the near future.

METHODS

Materials. D-ND powder and SYP 0-0.05 diamond powder of type Ib were obtained from Gansu Ling Yun Nano-Material Co., Ltd. (Lanzhou, China) and Van Moppes & Sons (Geneva, Switzerland), respectively. All the reagents used in this study were reagent grade. Solvents were dried according to standard procedures. Distilled water was used.

Functionalization. The setup depicted in Figure 1 was employed for the reactions with an ultrasonic processor (Branson, Ultrasonic-Homogenizer Sonifier II W-450 with a 5 mm microtip EDP No. 101-148-069 operated at the output control 2). For BASD treatments, the reactor was charged with 10 g of zirconia beads (Tosoh Co., YTZ Grinding Media, 0.05 mm). A round-bottom flask with a magnetic stirring bar was used for the MS reactions. Silanization was achieved on borane-reduced diamond surfaces[35] for D-NDs. SYP-NDs were silanized without the reduction step; 0.5 mL of (3-acryloxypropyl)trimethoxysilane in 7.0 mL of dry THF was added to 200 mg of reduced diamond powder. The mixture was agitated for 10 h at room temperature under nitrogen atmosphere with BASD, BLS, or MS. ZrO_2 and/or Ti in the BASD and BLS samples were removed by centrifugation. Dried powder was obtained after removal of silane by five consecutive washing/centrifugation cycles with acetone.

Arylation of diamond powder was performed by adding 2 g of aminobenzoic acid and 1 mL of amyl nitrite to 10 mL of an aqueous diamond suspension containing 300 mg of diamond and agitating for 15 h at 80 °C under ambient atmosphere with BASD, BLS, or MS. The products were subjected to consecutive

washing/centrifugation cycles in acetone using an ultrasound bath until the supernatants became colorless. In the case of BASD- and BLS-treated samples, ZrO_2 and/or Ti were then removed by centrifugation in ethanol. Subsequently, acetone-insoluble byproduct was removed using concentrated NaOH solution with consecutive washing/centrifugation cycles until the supernatants became colorless. Finally, the products were purified by consecutive washing/centrifugation cycles in water and subsequent dialysis (Medicell International Ltd., molecular weight cut-off 12 000−14 000 Da).

Heat treatments prior to arylation were performed at 1100 °C ($<10^{-3}$ mbar) for 1 h. The BASD pretreatment was carried out in 10 mL of distilled water with 10 g of zirconia beads at the maximum amplitude (output control 7) of the sonicator with cooling water applied to the reactor's outer walls.

Characterization. The particle size distributions and ζ potentials of the colloids were analyzed by DLS (Otsuka Electronics Co., Particle Analyzer FPAR-1000) using the Marquardt method and laser Doppler electrophoresis (Brookhaven Instruments Co., Zeta Plus/Beckman Coulter Inc., DelsaNano C), respectively. In the case of silanized samples, those measurements were made without removal of the unreacted silane in order to avoid condensation reactions upon removal. Microscopy was carried out in a high-resolution transmission electron microscope (FEI Company, Tecnai G2) with a field-emission electron gun operating at 300 kV. The FT-IR spectra of the purified samples were measured in a homemade vacuum cell equipped with NaCl optical windows (see Supporting Information, Figure S6) by using an FT-IR spectrometer (Perkin-Elmer Inc., Paragon 1000/Bruker Co., Vector 22) after heating the samples for 3 h at 150 °C *in vacuo* in order to remove the considerable amount of adsorbed water[46] (the silanized samples were dried at 120 °C because of condensation taking place at a higher temperature).

Acknowledgment. The authors acknowledge funding support from the Deutsche Forschungsgemeinschaft and the European Commission under the 6th Framework Programme (Nano4Drugs, EQUIND). We are grateful to N. Stock and S. Ziesmer for access to the ζ potential analysers, C. Näther and I. Jess for help with thermal analysis, and W. Bensch and J. Wang for access to EDX analysis (all Institute for Inorganic Chemistry, Kiel University, Germany).

Supporting Information Available: Additional figures, experimental procedures, and analytical data. This material is available free of charge *via* the Internet at http://pubs.acs.org.

REFERENCES AND NOTES

1. Biju, V.; Itoh, T.; Anas, A.; Sujith, A.; Ishikawa, M. Semiconductor Quantum Dots and Metal Nanoparticles: Syntheses, Optical Properties, And Biological Applications. *Anal. Bioanal. Chem.* **2008**, *391*, 2469–2495.
2. Eijkel, J. C. T.; van den Berg, A. Nanofluidics: What Is It and What Can We Expect from It? *Microfluid. Nanofluid.* **2005**, *1*, 249–267.
3. Balazs, A. C.; Emrick, T.; Russell, T. P. Nanoparticle Polymer Composites: Where Two Small Worlds Meet. *Science* **2006**, *314*, 1107–1110.
4. Ozin, G. A.; Arsenault, A. C. *Nanochemistry: A Chemical Approach to Nanomaterials*; Royal Society of Chemistry: Cambridge, UK, 2005.
5. Whitesides, G. M.; Grzybowski, B. Self-Assembly at All Scales. *Science* **2002**, *295*, 2418–2421.
6. Li, D.; Kaner, D. R. B. Shape and Aggregation Control of Nanoparticles: Not Shaken, Not Stirred. *J. Am. Chem. Soc.* **2006**, *128*, 968–975.
7. Vesaratchanon, S.; Nikolov, A.; Wasan, D. T. Sedimentation in Nano-Colloidal Dispersions: Effects of Collective Interactions and Particle Charge. *Adv. Colloid Interface Sci.* **2007**, *268*, 134–135.
8. Kuchibhatla, S. V. N. T.; Karakoti, A. S.; Seal, S. Colloidal Stability by Surface Modification. *JOM* **2005**, *57*, 52–56.
9. Vaisman, L.; Wagner, H. D.; Marom, G. the Role of Surfactants in Dispersion of Carbon Nanotubes. *Adv. Colloid Interface Sci.* **2006**, *128−130*, 37–46.
10. Xu, X.; Yu, Z.; Zhu, Y.; Wang, B. Effect of Sodium Oleate Adsorption on the Colloidal Stability and Zeta Potential of Detonation Synthesized Diamond Particles in Aqueous Solutions. *Diamond Relat. Mater.* **2005**, *14*, 206–212.
11. Niederberger, M.; Garnweitner, G.; Krumeich, F.; Nesper, R.; Cölfen, H.; Antonietti, M. Tailoring the Surface and Solubility Properties of Nanocrystalline Titania by a Nonaqueous *In Situ* Functionalization Process. *Chem. Mater.* **2004**, *16*, 1202–1208.
12. Sanchez, C.; de A. A. Soler-Illia, G. J.; Ribot, F.; Lalot, T.; Mayer, C. R.; Cabuil, V. Designed Hybrid Organic−Inorganic Nanocomposites from Functional Nanobuilding Blocks. *Chem. Mater.* **2001**, *13*, 3061–3083.
13. Wang, Y. A.; Li, J. J.; Chen, H.; Peng, X. Stabilization of Inorganic Nanocrystals by Organic Dendrons. *J. Am. Chem. Soc.* **2002**, *124*, 2293–2298.
14. White, M. A.; Johnson, J. A.; Koberstein, J. T.; Turro, N. J. toward the Synthesis of Universal Ligands for Metal Oxide Surfaces: Controlling Surface Functionality through Click Chemistry. *J. Am. Chem. Soc.* **2006**, *128*, 11356–11357.
15. Daniel, M.-C.; Astruc, D. Gold Nanoparticles: Assembly, Supramolecular Chemistry, Quantum-Size-Related Properties, and Applications towards Biology, Catalysis, and Nanotechnology. *Chem. Rev.* **2004**, *104*, 293–346.
16. Banerjee, S.; Hemraj-Benny, T.; Wong, S. S. Covalent Surface Chemistry of Single-Walled Carbon Nanotubes. *Adv. Mater.* **2005**, *17*, 17–29.
17. Han, X.; Li, Y.; Wu, S.; Deng, Z. a General Strategy Towards pH-Controlled Aggregation: Dispersion of Gold Nanoparticles and Single-Walled Carbon Nanotubes. *Small* **2008**, *4*, 326–329.
18. Marković, S.; Mitrić, M.; Starčević, G.; Uskoković, D. Ultrasonic De-agglomeration of Barium Titanate Powder. *Ultrason. Sonochem.* **2008**, *15*, 16–20.
19. Vasylkiv, O.; Sakka, Y. Synthesis and Colloidal Processing of Zirconia Nanopowder. *J. Am. Ceram. Soc.* **2001**, *84*, 2489–2494.
20. Pacek, A. W.; Utomo, P. D. A. Effect of Energy Density, pH and Temperature on De-Aggregation in Nano-Particles/Water Suspensions in High Shear Mixer. *Powder Technol.* **2007**, *173*, 203–210.
21. Muller, F.; Peukert, W.; Polke, R.; Stenger, F. Dispersing Nanoparticles in Liquids. *Int. J. Miner. Process.* **2004**, *74S*, S31–S41.
22. Seekkuarachchi, I. N.; Tanaka, K.; Kumazawa, H. Dispersion Mechanism of Nano-Particulate Aggregates Using a High Pressure Wet-Type Jet Mill. *Chem. Eng. Sci.* **2008**, *63*, 2341–2366.
23. Sauter, C.; Schuchmann, H. P. High Pressure for Dispersing and Deagglomerating Nanoparticles in Aqueous Solutions. *Chem. Eng. Technol.* **2007**, *30*, 1401–1405.
24. Chang, J.-Y.; Wu, H.-Y.; Hwang, G. L.; Su, T.-Y. Ultrasonication-Assisted Surface Functionalization of Double-Walled Carbon Nanotubes with Azobis-Type Radical Initiators. *J. Mater. Chem.* **2008**, *18*, 3972–3976.
25. Krüger, A.; Ozawa, M.; Kataoka, F.; Fujino, T.; Suzuki, Y.; Aleksenskii, A. E.; Vul', A. Ya.; Osawa, E. Unusually Tight Aggregation in Detonation Nanodiamond: Identification and Disintegration. *Carbon* **2005**, *43*, 1722–1730.
26. Inkyo, M.; Tahara, T.; Iwaki, T.; Iskandar, F.; Hogan, C. J., Jr.; Okuyama, K. Experimental Investigation of Nanoparticle Dispersion by Beads Milling with Centrifugal Bead Separation. *J. Colloid Interface Sci.* **2006**, *304*, 535–540.
27. Sommer, M.; Stenger, F.; Peukert, W.; Wagner, N. J. Agglomeration and Breakage of Nanoparticles in Stirred Media Mills: A Comparison of Different Methods and Models. *Chem. Eng. Sci.* **2006**, *61*, 135–148.
28. Voronov, A.; Kohut, A.; Synytska, A.; Peukert, W. Mechanochemical Modification of Silica with Poly(1-vinyl-2-pyrrolidone) by Grinding in a Stirred Media Mill. *J. Appl. Polym. Sci.* **2007**, *104*, 3708–3714.
29. Schmidt, H.; Tabellion, F.; Schmitt, K.-P.; Oliveira, P.-W. Ceramic Nanomaterials and Nanotechnology II. *Ceram. Trans.* **2004**, *48*, 173–186.

30. Ozawa, M.; Inakuma, M.; Takahashi, M.; Kataoka, F.; Krueger, A.; Osawa, E. Preparation and Behavior of Brownish, Clear Nanodiamond Colloids. *Adv. Mater.* **2007**, *19*, 1201–1206.
31. Shenderova, O. A.; Zhirnov, V. V.; Brenner, D. W. Carbon Nanostructures. *Crit. Rev. Solid State Mater. Sci.* **2002**, *27*, 227–356.
32. Osawa, E. Recent Progress and Perspectives in Single-Digit Nanodiamond. *Diamond Relat. Mater.* **2007**, *16*, 2018–2022.
33. Xu, K.; Xue, Q. Deaggregation of Ultradispersed Diamond from Explosive Detonation by a Graphitization: Oxidation Method and by Hydroiodic Acid Treatment. *Diamond Relat. Mater.* **2007**, *16*, 277–282.
34. Barnard, A. S. Self-Assembly in Nanodiamond Agglutinates. *J. Mater. Chem.* **2008**, *18*, 4038–4041.
35. Krüger, A.; Liang, Y.; Jarre, G.; Stegk, J. Surface Functionalisation of Detonation Diamond Suitable for Biological Applications. *J. Mater. Chem.* **2006**, *16*, 2322–2328.
36. Raty, J.-Y.; Galli, G. Ultradispersity of Diamond at the Nanoscale. *Nat. Mater.* **2003**, *2*, 792–795.
37. Fang, X. W.; Mao, J. D.; Levin, E. M.; Schmidt-Rohr, K. Nanoaromatic Core−Shell Structure of Nanodiamond from Solid-State NMR Spectroscopy. *J. Am. Chem. Soc.* **2009**, *131*, 1426–1435.
38. Kuznetsov, V. L.; Chuvilin, A. L.; Butenko, Y. V.; Mal'kov, I. Yu.; Titov, V. M. Onion-like Carbon from Ultra-Disperse Diamond. *Chem. Phys. Lett.* **1994**, *222*, 343–348.
39. Barnard, A. S.; Sternberg, M. Crystallinity and Surface Electrostatics of Diamond Nanocrystals. *J. Mater. Chem.* **2007**, *17*, 4811–4819.
40. Eidelman, E. D.; Siklitsky, V. I.; Sharonova, L. V.; Yagovkina, M. A.; Vul', A. Ya.; Takahashi, M.; Inakuma, M.; Ozawa, M.; Osawa, E. A Stable Suspension of Single Ultrananocrystalline Diamond Particles. *Diamond Relat. Mater.* **2005**, *14*, 1765–1769.
41. Panich, A. M.; Shames, A. I.; Vieth, H.-M.; Osawa, E.; Takahashi, M.; Vul', A. Ya. Nuclear Magnetic Resonance Study of Ultrananocrystalline Diamonds. *Eur. J. Phys. B* **2006**, *52*, 397–402.
42. Raty, J.-Y.; Galli, G.; Bostedt, C.; van Buuren, T. W.; Terminello, L. J. Quantum Confinement and Fullerenelike Surface Reconstructions in Nanodiamonds. *Phys. Rev. Lett.* **2003**, *90*, 037401.
43. Shima, A. Studies on Bubble Dynamics. *Shock Waves* **1997**, *7*, 33–42.
44. Doktycz, S. J.; Suslick, K. S. Interparticle Collisions Driven by Ultrasound. *Science* **1990**, *247*, 1067–1069.
45. Makino, K.; Mossoba, M. M.; Riesz, P. Chemical Effects of Ultrasound on Aqueous Solutions. Evidence for ·OH and ·H by Spin Trapping. *J. Am. Chem. Soc.* **1982**, *104*, 3537–3539.
46. Ji, S.; Jiang, T.; Xu, K.; Li, S. FTIR Study of the Adsorption of Water on Ultradispersed Diamond Powder Surface. *Appl. Surf. Sci.* **1998**, *133*, 231–238.